

Characteristic Temperature Relationship with Laser Cavity Length of Mid-IR Pbse/Pbsrse MQW Structure

Majed Khodr

Department of Electronics and Communications Engineering,
American University of Ras Al Khaimah,
United Arab University Ras Al Khaimah, P.O. Box 10021, United Arab Emirates

Abstract: The current research efforts are focused on development of practical mid-IR laser devices that can be used in high resolution spectrometers for sensitive detection of specific gas molecules. Improvements in processing and thermal management are expected to yield room temperature lasing in the near future. In this research, the effects of laser cavity length on a critical thermal operational parameter, the characteristic Temperature (T_0) was studied for this PbSe/Pb_{0.934}Sr_{0.066}Se mid-IR quantum well structure at three temperature ranges $77 < T < 150$ K, $150 < T < 300$ K and $77 < T < 300$ K. It was noticed that T_0 is high for short cavity lengths then decreases to an almost constant value after some critical length of 100 μ m. The effects of quantum efficiency were noticeable for short cavity lasers with a reduction of 55-62% in T_0 for the $77 \text{ K} \leq T \leq 150 \text{ K}$ and $150 \text{ K} \leq T \leq 300 \text{ K}$ and 68-73% for the $150 \text{ K} \leq T \leq 300 \text{ K}$ range. However, as the cavity lengths increased above the critical value the effects are almost constant. The data were best fitted to a second degree polynomials which can be used to determine the characteristic temperature values as a function of cavity length.

Key words: Characteristic temperature, cavity length, quantum efficiency, PbSe, PbSrSe

INTRODUCTION

Recently, demonstrated CW laser mission from IV-VI semiconductor quantum well material at heat sink temperatures up to 275 K (Eibelhuber *et al.*, 2009, 2010). As quoted from Eibelhuber (2010) "This proves the feasibility of room temperature type-I interband lasing at long wavelengths and opens the way for low-cost mid-infrared laser sources on readily available thermoelectric coolers for various applications. Further, improvements in processing and thermal management are expected to yield room temperature lasing in the near future. The current research efforts in this field are focused on development of practical mid-IR laser devices that can be used in high resolution spectrometers for sensitive detection of specific gas molecules. These efforts will build upon prior work performed by the investigators in the fields of thin film IV-VI semiconductor epitaxial layer growth, optoelectronic device materials processing and mid-IR materials and device characterization. Moreover, they will involve further improvements in processing, optimization of active region material and device design and development of innovative methods to achieve better thermal management.

Better thermal management requires investigations and knowledge of the important critical characteristic Temperature (T_0) parameter. Higher characteristic

temperatures values imply that the threshold current density and the external differential quantum efficiency of the device increase less rapidly with increasing temperatures. This translates into the laser being more thermally stable.

In previous publications, the characteristic temperature calculations and dependency on quantum efficiency was analyzed for Pb_{0.934}Sr_{0.066}Se multiple quantum well structure at three temperature ranges; $77 \text{ K} \leq T_0 \leq 150 \text{ K}$, $150 \leq T_0 \leq 300 \text{ K}$ and $77 \text{ K} \leq T_0 \leq 300 \text{ K}$. In this research, we continue these efforts and investigate the effects of laser cavity on the characteristic temperature values in the above three temperature ranges. Moreover, we will estimate the critical lengths values after which the characteristic temperatures remains almost constant. The effects of quantum efficiency on these critical cavity lengths will be included.

MATERIALS AND METHODS

The optical analysis of PbSe/Pb_{0.934}Sr_{0.066} single quantum well lasers is done based on the formulas published earlier for IV-VI semiconductor materials (Khodr, 2013; Khodr and McCann, 2014). The index of refraction for the well material PbSe is 4.86 and the index of refraction for the barrier material Pb_{0.934}Sr_{0.066}Se is 4.38 and they are considered in this work independent of

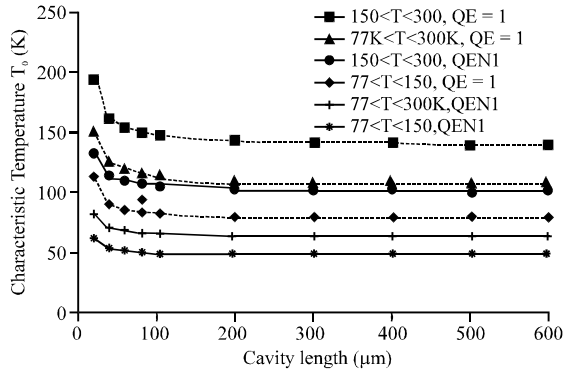


Fig. 1: The dashed curves are for $\eta = 1$ and the solid curves for $\eta \neq 1$

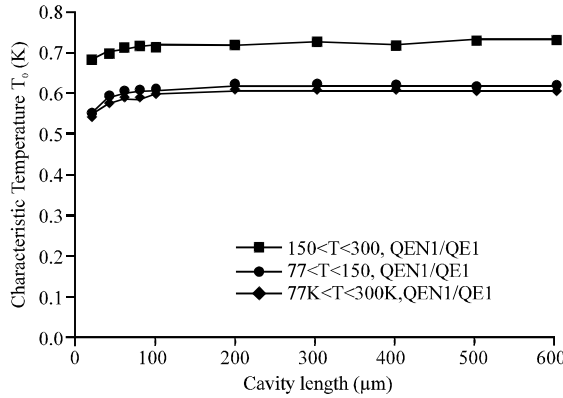


Fig. 2: The ratio of characteristic temperatures of $\eta \neq 1$ to $\eta = 1$

wavelength and temperature. The thickness of the well material is 7 nm, the thickness of the barrier material is 70 nm and the number of wells is 7.

The threshold current density J_{th} that corresponds to the modal gain value that satisfies the oscillation condition can be obtained from the modal gain-current density plots. The temperature dependence of the threshold current density J_{th} depends on the temperature dependence of the gain, internal losses and quantum efficiency (η). Inclusion of Auger recombination in addition to the temperature dependence of the gain in the calculations of J_{th} results in a temperature variation as $\exp(T/T_0)$ where T_0 is the characteristic temperature in a specific temperature range (Findlay *et al.*, 1998).

We studied the relationship between the characteristic Temperature (T_0) and laser cavity Length (L) in three temperature ranges; $77\text{ K} \leq T \leq 150\text{ K}$, $150 \leq T \leq 300\text{ K}$ and $77\text{ K} \leq T \leq 300\text{ K}$. The data for both the assumed quantum efficiency value of one and for the theoretically calculated quantum efficiency were plotted in Fig. 1 for the three temperature ranges. The dotted lines represent

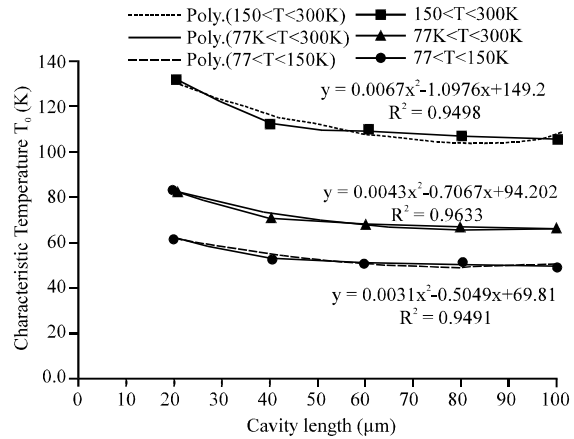


Fig. 3: T_0 values in the cavity range $20\ \mu\text{m} \leq L \leq 100\ \mu\text{m}$, the best fitted polynomials and correlation coefficients squares are included above each curve ($\eta \neq 1$)

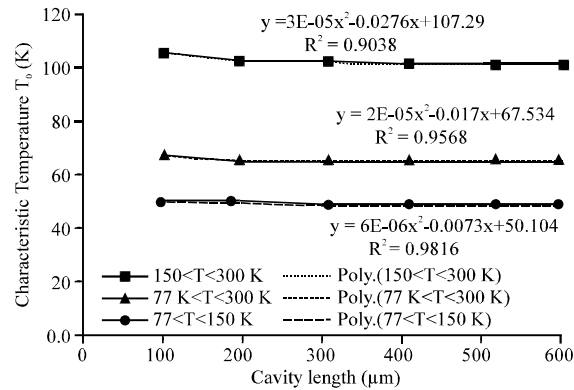


Fig. 4: The T_0 values in the range $100\ \mu\text{m} \leq L \leq 600\ \mu\text{m}$, the best fitted polynomials and correlation coefficients squares are included above each curve ($\eta \neq 1$)

unity quantum efficiency and the solid lines represent the theoretical quantum efficiency. In Fig. 2, we plotted the data that represents the ratio of T_0 values including the theoretical quantum efficiency to those values with unity quantum efficiency as a function of cavity length range from 20-600 μm . Finally, we divided the total cavity length range into two parts, the first one from $20\ \mu\text{m} \leq L \leq 100\ \mu\text{m}$ and the second part from $100\ \mu\text{m} \leq L \leq 600\ \mu\text{m}$ and plotted the data as shown in Fig. 3 and 4, respectively. The reason for this is to be able to best fit the data in each range as shown in the figures, something, we were unable to do if we combined the two ranges. Each of the three plots represents one of the three temperature ranges of interest.

RESULTS AND DISCUSSION

As noticed from Fig. 1, including quantum efficiency lowers the characteristic temperature values for all cavity lengths in all of the three different temperature ranges. From both curves, one notice that the characteristic temperature is high for short cavity lengths then decreases to an almost constant value after some critical cavity length. The effects of including the quantum efficiency are noticed in Fig. 2 where the curve for the $77\text{ K} \leq T \leq 150\text{ K}$ is much lower than the curve for the $150\text{ K} \leq T \leq 300\text{ K}$ range. The data for the total range $77\text{ K} \leq T \leq 300\text{ K}$ is closer to the low temperature range and this suggests that there is a leakage current in this range that needs to be added to the calculations. This leakage current was calculated in previous publication (Khodr and McCann, 2014). It is also noticeable the effects of quantum efficiency for short cavity lasers, however as the cavity length increased above a critical value the effects are almost constant. Figure 2 clearly show a reduction of 55-62% in T_0 for the $77\text{ K} \leq T \leq 150\text{ K}$ and $150\text{ K} \leq T \leq 300\text{ K}$ and 68-73% for the $150\text{ K} \leq T \leq 300\text{ K}$ range. The percentage for reduction for all three temperature ranges is smaller for the short cavity and increases to a constant value after a critical cavity length.

To determine these critical values, we divided and best fitted the data in two ranges $20\text{ }\mu\text{m} \leq L \leq 100\text{ }\mu\text{m}$ and $100\text{ }\mu\text{m} \leq L \leq 600\text{ }\mu\text{m}$ and the results are shown in Fig. 3 and 4, respectively. The best fit formulas for the data was found to be of second degree polynomials shown above each curve in these figures. In the text here, we list two of these equations that are obtained for the total temperature range of $77\text{ K} \leq T \leq 300\text{ K}$. For $20\text{ }\mu\text{m} \leq L \leq 100\text{ }\mu\text{m}$:

$$T_0 = 4.3 \times 10^{-3} L^2 - 0.707L + 94.202 \quad (R^2 = 0.9633) \quad (1)$$

For $100\text{ }\mu\text{m} \leq L \leq 600\text{ }\mu\text{m}$:

$$T_0 = 2 \times 10^{-5} L^2 - 0.017L + 67.534 \quad (R^2 = 0.9568) \quad (2)$$

CONCLUSION

We studied and analyzed the effects of cavity length on the characteristic temperature. The characteristic temperature is high for short cavity lengths then decreases to an almost constant value after some critical cavity length of $100\text{ }\mu\text{m}$. It was found that inclusion of the quantum efficiency decreases the characteristic temperature by 60% for a wide range of cavity lengths and this suggests that there is a leakage current that needs to be added to the calculations. The best fit formulas for the data were second degree polynomials. These formulas can be used to predict the characteristic temperature of the device as a function of cavity length.

REFERENCES

- Eibellhuber, M., T. Schwarzl, G. Springholz and W. Heiss, 2009. Lead salt microdisk lasers operating in continuous wave mode at 5.3 μm wavelength. *Appl. Phys. Lett.*, 94: 021118-021118.
- Eibellhuber, M., T. Schwarzl, S. Pichler, W. Heiss and G. Springholz, 2010. Near room temperature continuous-wave laser operation from type-I interband transitions at wavelengths beyond 4 μm . *Appl. Phys. Lett.*, 97: 1-3.
- Findlay, P.C., C.R. Pidgeon, R. Kotitschke, A. Hollingworth, B.N. Murdin, C.J.G.M. Langerak and G. Springholz, 1998. Auger recombination dynamics of lead salts under picosecond free-electron-laser excitation. *Phys. Rev. B.*, 58: 12908-12908.
- Khodr, M., 2013. Effects of quantum efficiency on PbSe/PbSrSe multiple quantum well structures. *Proceedings of the International Society for Optics and Photonics SPIE NanoScience+Engineering*, September 26, 2013, San Diego, California, United States, pp: 88160P-88160P.
- Khodr, M.F. and P.J. McCann, 2014. Theoretical analysis and design of PbSe/PbSrSe quantum well structures for fabricating tunable mid-infrared lasers. *Intl. J. Appl. Eng. Res.*, 9: 4065-4081.